

# Miniature Monitoring System for Environmental Indicators and Physiological Signs

LIN Yu-ke

*School of Electrical Engineering and Automation,  
Henan Polytechnic University, Jiaozuo454003, China*

---

**Abstract:** Due to work-related reasons, people's physical health is receiving increasing attention, and the trend of major diseases affecting younger individuals is on the rise with each passing year. As the environment is closely linked to personal physical well-being, it is crucial for individuals to pay attention to environmental indicators while monitoring their own physiological data. Therefore, the real-time and convenient detection of environmental indicators and individuals' physiological health status, along with timely provision of preventive or medical advice, has become an urgent issue. This paper explores a miniaturized monitoring system that allows users to monitor environmental and physiological responses. The system comprises three components: a sensor signal acquisition module, a main control chip module, and an Android application. Experimental results demonstrate that this monitoring system meets design requirements and achieves the expected effects.

**Keywords:** Android; miniature; Stm32; environmental and physiological monitoring; embedded system.

---

## I. Introduction

In recent years, amidst the rapid economic growth, individuals are encountering escalating competition in their daily lives, leading to mounting psychological pressures<sup>[1]</sup>. This trend has not only resulted in an increase in the incidence of sudden death but also a shift towards younger age groups, posing a significant threat to the health of young people<sup>[2]</sup>. Experts have noted that the fast-paced lifestyle of modern society has made staying up late a common occurrence, fostering irregular living habits<sup>[3]</sup>. Moreover, due to the consistent exposure to a fixed environment, the need for continuous monitoring of physiological signs and environmental indicators has become increasingly crucial for high-risk individuals, evolving into a routine behavior.

Miniature monitoring devices, in comparison to traditional physiological monitoring instruments, possess advantages such as compact size, portability, and ease of operation<sup>[4]</sup>. While they may not match the functionality and performance of large, advanced medical monitoring equipment used in hospitals, their low cost and affordability lend them suitable for widespread adoption among the general population, thereby drawing more attention from research scholars<sup>[5]</sup>. As early as 2003, the University of Zurich developed the world's first wearable medical alert and monitoring system<sup>[6]</sup>. During the research on the home digital medical monitoring system project, the Third Military Medical University also developed a palmtop computer-based portable ECG and blood pressure monitor<sup>[7]</sup>. In addition, numerous research institutions and technology companies have introduced products capable of monitoring various physiological indicators<sup>[8]</sup>. However, these products often suffer from issues like bulky size and complex operation. The emergence of wearable fitness trackers has opened up new horizons for this industry to reach a wider user base. Wearable fitness trackers are also capable of collecting various physiological metrics, such as heart rate, body temperature, energy expenditure, and step count, and connect with smartphones via Bluetooth for data transmission and display<sup>[9]</sup>. Wearable fitness trackers offer users the convenience of portability and simplicity of operation<sup>[10]</sup>. Despite their long standby time, the need for periodic charging can still be inconvenient for users. In recent years, with the widespread adoption of smartphones, physiological monitoring systems have gradually been integrated into mobile phones. For instance, in 2014, Samsung's flagship Galaxy S5 smartphone was equipped with a heart rate monitoring function, but its high price made it inaccessible to average users.

This paper proposes the design of a miniature environmental indicator and human physiological data monitor based on the Android platform. This system embeds various physiological sensors and environmental sensors to collect and convert biometric data and environmental indicators, facilitating data transmission through the USB port of a smartphone. The smartphone then displays the received data information on a mobile application (APP) and enables timely warning and alert functionalities.

## II. System

**Architecture Model** The miniature environmental indicator and human activity physiological response monitoring system comprises two major aspects: the hardware component and the Android client software component.

The hardware composition primarily consists of two parts: external environmental monitoring and human characteristic monitoring. Environmental monitoring encompasses light intensity monitoring and room temperature monitoring, while human characteristic monitoring focuses on capturing heart rate data, motion data, and body temperature data. The monitoring system is divided into two modes: a low-power consumption monitoring mode and a regular monitoring mode. In the low-power consumption mode, the system is powered by a 3.3v button battery and maintains minimal power consumption to collect data once per minute. Pressing the announcement button automatically broadcasts the current data. In the regular monitoring mode, the system connects to a smartphone for power supply. After the sensors collect data, they undergo analog-to-digital conversion and transmit the data to an internal storage chip. Upon establishing an OTG communication link with the smartphone, the real-time data is processed and displayed on the mobile app. Additionally, the STM32, a Cortex-M series core under the ARM architecture, is selected as the microcontroller unit (MCU). Compared to other products, it offers high performance, low cost, low power consumption, and stable operation in industrial manufacturing.

In the regular mode of the client software, if the monitored data exceeds a certain threshold, a pop-up window will appear to remind the user to pay attention to their physical condition and take appropriate rest. The backend database can store the measured data in real-time, allowing users to query historical data for convenient comparison of monitoring data before and after. This provides a clearer understanding of one's physical condition. Additionally, the data can be compared to public data to identify and distinguish subtle abnormalities, and to environmental data to provide targeted recommendations for the current environment.

It is important to note that the design of the circuit schematic needs to consider the complex electromagnetic environment encountered in daily use, as well as electromagnetic interference (EMI) between modules. Therefore, electromagnetic compatibility (EMC) design plays a crucial role in optimizing data acquisition accuracy and operational stability. The design must take into account the potential harm of electromagnetic radiation to humans, establish design requirements for EMI mitigation, and consider the impact of external electromagnetic fields on the internal system, setting forth design requirements for electromagnetic susceptibility (EMS). This paper proposes a standardized design for the system based on these considerations. The block diagram of the system's structure is illustrated in Figure 1.

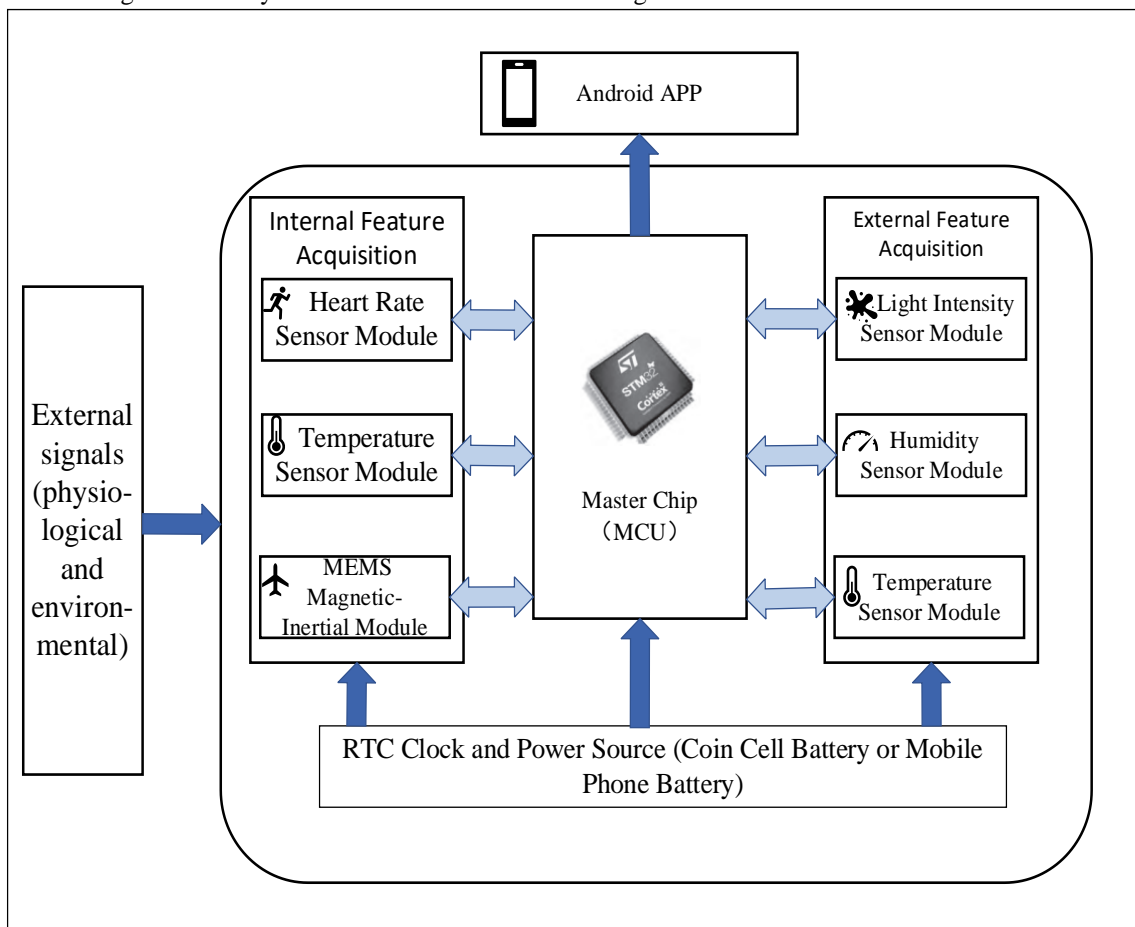


Figure 1. System Block Diagram

**2.1 System Hardware Design**

The environmental indicator and human physiological response monitoring system primarily encompasses data acquisition by sensor modules, data conversion and output, as well as data display.

The environmental indicator and human physiological response monitoring system utilizes various sensor modules to acquire voltage signals representing body temperature, room temperature, humidity, light intensity, and heart rate. These signals are obtained through a body temperature sensor module, a light intensity sensor module, a humidity sensor module, a MEMS attitude sensor, and a heart rate sensor module. An AD converter digitizes the signals and transmits them to a microcontroller for processing. The data signals are then temporarily stored in memory and transmitted to a connected smartphone via OTG connection, where they are displayed via an Android application.

In this paper, the MAX30102 heart rate sensor module is used for heart rate acquisition, the MAX30205 body temperature sensor module for temperature acquisition, the MPU9250 inertial sensor and HMC5883L magnetic sensor for posture and movement detection, the DHT11 temperature and humidity sensor for ambient environmental conditions, and the BH1750 light intensity sensor for light intensity acquisition.

The physiological monitoring system primarily focuses on data acquisition, conversion, transmission, and display from three major sensor modules. The system composition and functional structure are illustrated in Figure 2. Through the body temperature sensor module, light intensity sensor module, and heart rate sensor module, voltage signals representing body temperature, light intensity, and heart rate are obtained. The AD converter digitizes these signals and transmits them to the microcontroller for processing. The processed data signals are then transmitted to the connected smartphone, where they are displayed via the Android application.

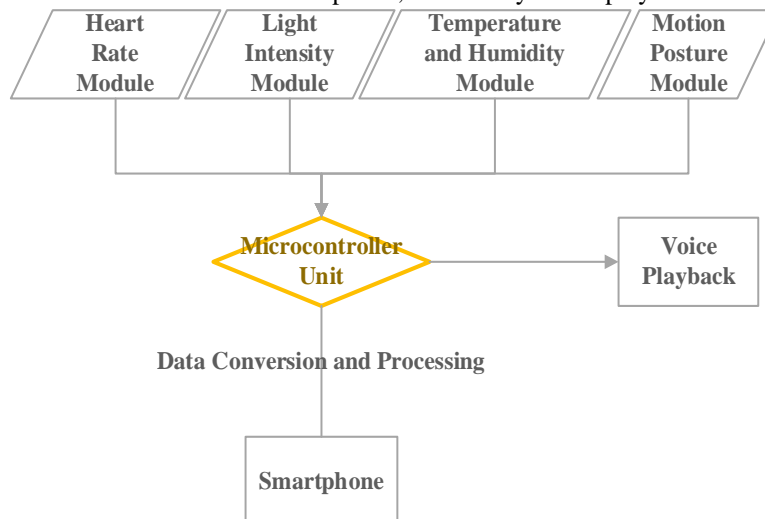


Figure 2. Composition and Functional Block Diagram

Utilizing the external pin interrupt of the STM32F103RE microcontroller's General-Purpose Input/Output (GPIO) pins, the system captures the rising edges of sensor signals to achieve feature and environmental detection. In the design, rising edge sampling is chosen for the interrupts, with the sampling frequency set to 1 sample per minute in low-power mode to conserve energy. After sampling, the modules enter a low-power sleep state, awaiting the next wake-up trigger from the RTC (Real-Time Clock). In regular mode, the sampling frequency is set to 100 samples per second. Due to the presence of noise in the sensor data during operation, including random noise, vibration noise, and geomagnetic noise, as well as errors such as zero bias and scale factor errors, there are integration biases when obtaining true values through integration. Therefore, further filtering is necessary. In this paper, an improved adaptive Kalman filter is utilized to process the errors, resulting in sensor data with acceptable levels of confidence.

**2.2 System software design**

The software application platform chosen for this paper is the Android system, which boasts a wide range of applicability and the advantages of cross-platform convenience and flexible portability. Given that the MCU selected in this paper does not include an external storage chip, and the internal storage space of the main control chip is quite limited, it is decided to place most of the storage and computation tasks on the Android mobile device to address the issues of slow runtime scheduling and limited storage space. In the design approach presented here, the device side is responsible only for real-time data acquisition and minimal data

storage, effectively reducing the device's computational requirements and physical size, thereby greatly enhancing the portability of the external environment monitoring system.

The software design of the physiological monitoring system is divided into three parts: heart rate detection, body temperature detection, and light intensity detection. When users open the physiological characteristics section of the Android application on their mobile phones, they are presented with three options corresponding to these three functions. After connecting the physiological monitoring system to the phone, users can select the desired detection function based on their needs. For example, if they choose heart rate or body temperature detection, the corresponding test values will be displayed on the phone screen after the test begins. If the test results exceed a certain threshold, a pop-up notification will be triggered. Additionally, users can also query and delete historical data. If light intensity detection is chosen, the detected value will be displayed on the phone screen after the test begins, and a pop-up notification will be triggered if it exceeds a specified limit. All data saved in memory under low-power mode is transmitted via OTG and ultimately recorded in the phone's database.

The system database is designed to store detected heart rate and body temperature values. Users can store real-time data during heart rate and body temperature detection, enabling them to compare current data with previously detected data to gain a clearer understanding of their health status. The database view is presented in a list format, displaying the detected heart rate and body temperature values along with the current detection time. Adapters are defined for the heart rate and body temperature data lists, enabling the data stored in the database to be displayed in a list format. Regarding database operations, methods for storing, retrieving, and deleting data from the heart rate and body temperature tables are defined. Users can view and delete historical data on the data display page of the database. The subsequent paragraphs you send will be translated in accordance with the conventions of English academic papers.

### 2.3

### 2.4 Application scenarios

Compared to commonly used sports wristbands, the product designed in this paper aims to minimize space occupation by not including additional Bluetooth and rechargeable batteries. For most of the daily use, the low-power mode is powered by a button battery, and when connected to a phone via OTG, it is powered by the phone itself. The circuit design utilizes a four-layer board, enabling a compact and portable device size while ensuring reliable performance and basic functionality. In the anticipated usage scenarios, it can be encapsulated into thumb rings, necklaces, and other accessories, freeing users from being constrained to wearing it on the wrist due to battery and display considerations.

The current design space is 4cm x 6cm x 1.5cm, and further optimization of the PCB circuit layout will further reduce the occupied space. Therefore, various packaging options are available to create exquisite shapes, with the recommended packaging shape illustrated in Figure 3.



Figure 3. Packaging Style

### III. Algorithm Mathematical Model

To address the shortcomings of traditional Kalman filtering in handling rapid multi-valued problems, which often fail to reflect realistic usage scenarios, we have introduced adaptive Kalman filtering with modifications. Specifically, we have integrated the GM(1,1) model to leverage multiple data points for more accurate predictions. Additionally, we have employed the dung beetle algorithm to optimize the gray model, aiming to better adapt to sensor data.

In the final process of calculating the drilling attitude through integration, we have chosen to utilize an adaptive feedback network for correcting the integration process. Furthermore, the dung beetle algorithm has been applied to achieve adaptivity through optimization.

Gray prediction is a method used to forecast systems that contain both known and uncertain information. It focuses on predicting gray processes that vary within a certain range and are time-dependent, making it suitable for scenarios where the correlation between different data points is weak. The GM(1,1) model refers to a first-order differential equation model with a single variable. Its application involves using the original non-negative data sequence, weakening randomness through accumulation or similar methods, obtaining a regular discrete data sequence, establishing a corresponding differential equation model, deriving solutions at discrete points, and finally estimating the original data through cumulative reduction, thus achieving prediction of the original data.

#### 3.1 Data Preprocessing

For error handling in data, residual testing is employed, specifically residual normality testing: This is done to determine if the noise errors in the data conform to a normal distribution, and thus a residual normality test is performed on the data.

$$0 < \left| \sum_1^n (X_{n+1} - X_n) \right| < lb \tag{1}$$

In the equation, represents the nth data point, and lb is the upper limit of the tolerable error. When the test is passed, it determines that the residuals follow a normal distribution, and then the next step is to check whether the residuals conform to the specifications:

$$ub < 1 - \left| \frac{(X_{n+1} - X_n)}{(X_n - X_{n-1})} \right| < 1 \tag{2}$$

In the equation,  $X_n$  represents the nth data point, and ub stands for the upper limit of the tolerable error. Any data that exceeds this limit is considered as excessively large error data, and an empirical value of 0.5 is often chosen for ub.

#### 3.2 Constructing the GM (1,1) Model

For common non-negative time series, the expression of an exponential curve can be used to approximate the accumulated generation sequence. Correspondingly, a first-order ordinary differential equation can be constructed to solve for the functional expression that fits the exponential curve, which takes the form of:

$$\frac{dx^{(1)}}{dt} + ax^{(1)} = u \tag{3}$$

Since the data is discrete, to find  $X(1)$ , we need to solve for a and u. Therefore:

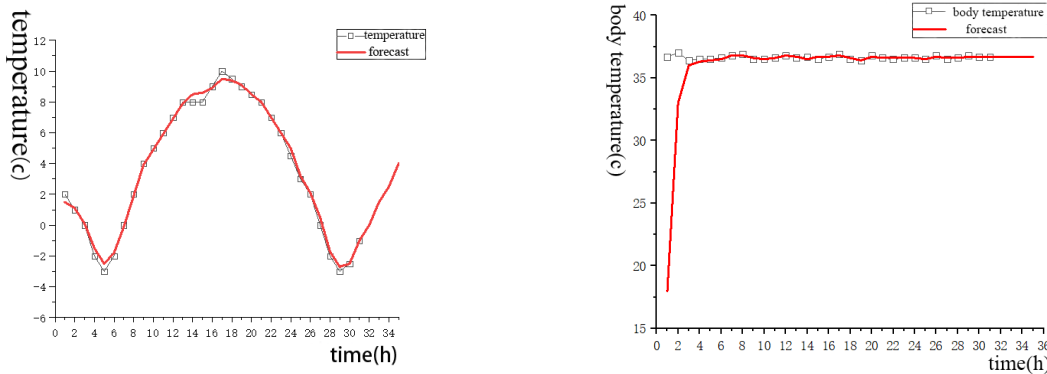
$$\frac{\Delta x^{(1)}}{\Delta t} = \Delta x^{(1)} = x^{(1)}(t) - x^{(1)}(t-1) = x^{(0)}t \tag{4}$$

$$x^{(0)}t + ax^{(1)}(t) = u \tag{5}$$

The matrix representation is:  $Y = X\beta + \delta$ , Using the least squares method for solving, we aim to minimize the sum of squared differences between the observed values and the estimated values.

By employing the GM(1,1) model, 34 data points are obtained, with 30 of them serving as the original data. These 30 data points are divided into groups of three, and the model is constructed three times using each group to predict five data points. Four of the predicted points undergo a difference ratio test with the corresponding data points from the original data. After passing the test, the fifth point is taken as the weighted average of the model's predicted values that have passed the test. Figure 4 illustrates the fitting and prediction of sensor data for a single set of measurements.

For each group of data, an arbitrary function is used for transformation, and the function is reversed to retrieve the data points after the prediction process is complete.



(a) Environmental Temperature Data Fitting (b) Human Body Temperature Data Fitting  
 Figure 4 Sensor Model Fitting Data

### 3.3 Model Validation and Iteration

The dung beetle algorithm is an optimization algorithm that mimics the behavior of dung beetle populations to find the optimal solution. The population is divided into four categories: rolling dung beetles, thief dung beetles, egg-laying dung balls, and small dung beetles. It simulates five types of behaviors of dung beetles: rolling dung, dancing, foraging, breeding, and stealing. Due to the high similarity between the population behavior of dung beetles and finding the optimal fitting data in a discrete space, the dung beetle algorithm is chosen for parameter optimization because of its high degree of dispersion, low quantity certainty, but high convergence.

To test the degree of fit of the model to the original data, a grade ratio deviation test is used: First, the original data grade ratio is calculated:

$$\varepsilon(K) = \frac{x^{(0)}(K)}{x^{(0)}(K-1)} \quad (K = 2, 3, \dots) \quad (6)$$

Calculate the grade ratio deviation and the average grade ratio deviation based on the development coefficient (-a):

$$\eta(k) = \left| 1 - \frac{1 - 0.5a}{1 + 0.5a} \frac{1}{\varepsilon(K)} \right| \quad (7)$$

If the average grade ratio deviation is less than or equal to 0.2, it is considered that the model achieves a general fit to the original data. If  $\bar{\eta}$  is less than 0.1, it is considered that the model has an excellent fitting effect on the data.

To adaptively improve the model, a population-based algorithm is used for optimization. The  $\bar{\eta}$  value from the above formula is set as the optimization objective function, with  $x$  representing the index of the data points. The optimization constraints are set as the spatial point set containing the data points.

### 3.4 True value validation

Based on the concept of using observations to correct the current value in the Kalman Filter algorithm, the final result is calculated using weighted averaging, in a form similar to:

$$x_i = x_i' + k_i (x^i - x_i') \quad (8)$$

To estimate the optimal data points for other groups using the current optimal data point, reducing the difficulty of repeatedly searching for the optimal parameter values, the process can be iterated repeatedly. However, due to the issues of insufficient smoothness and lack of significant correlation between the predicted data, a second-order residual correction can be applied to the data:

$$\Delta x_n = \frac{(\Delta x_n + \Delta x_{n+1})}{2} - \frac{(\Delta x_n - \Delta x_{n+1})}{2} \quad (9)$$

$$\Delta x_{n+1} = \frac{(\Delta x_n + \Delta x_{n+1})}{2} - \frac{(\Delta x_n - \Delta x_{n+1})}{2} \quad (10)$$

Given that the data exhibits the same second-order acceleration, it can be approximated as data points on a quadratic curve, thus completing the smoothness validation. This preparation sets the stage for using a neural network to discover the relationship parameters between the data points and the true values.

### 3.5 BP Neural Network Handling Integral Deviation

In the sensors utilized in this paper, as MEMS sensors acquire acceleration and angular velocity data, to obtain attitude paths, it is necessary to integrate the acceleration and angular acceleration data from the MEMS. However, during the integration process, every error accumulates, necessitating a mapping between the MEMS data and actual data. However, traditional methods of establishing mapping functions fail to meet the requirement of specific data processing for specific cases, for example:

$$x_n = x_{n-1} + k_1 v + k_2 v^2 + \Delta u \tag{11}$$

In this scenario, where the precision is second-order but the parameter values need to be calculated and include error values, in order to reduce such calculations and minimize errors, a BP (Backpropagation) neural network is established. This network structure constructs the mapping relationship between the data and the actual values.

## IV. System Testin

### 4.1 Analysis of System Performance Test Results

The system testing environment was set at a normal room temperature, with the mobile terminal running on its own Android operating system. The Android application for the physiological sign monitoring system was operated on a Meizu note1 phone. During the testing, the phone was connected to the monitoring system and powered by the phone itself. During the tests, multiple test events were switched on the main page, and the APP was able to navigate to the corresponding pages without any issues. An example of the initialization page for some feature data testing is shown in Figure 5.

heart rate&sport	< temperature&body temperature	< light&humidity
heart rate:96 state:running today's workout:3443	Temp: 23.3°C body: 36.6°C data:2024.2.1 4:10	HUM: 35% E: 433cd data:2024.2.1 4:46
heart rate:93 state:running today's workout:3370	Temp: 23.3°C body: 36.6°C data:2024.2.1 4:09	HUM: 37% E: 453cd data:2024.2.1 4:45
heart rate:95 state:running today's workout:3370	Temp: 23.4°C body: 36.5°C data:2024.2.1 4:08	HUM: 36% E: 446cd data:2024.2.1 4:44
heart rate:95 state:running today's workout:3301	Temp: 23.4°C body: 36.6°C data:2024.2.1 4:07	HUM: 36% E: 453cd data:2024.2.1 4:43
heart rate:96 state:running today's workout:3225	Temp: 23.3°C body: 36.5°C data:2024.2.1 4:06	HUM: 36% E: 451cd data:2024.2.1 4:42
heart rate:92 state:running today's workout:3147	Temp: 23.2°C body: 36.5°C data:2024.2.1 4:05	HUM: 37% E: 441cd data:2024.2.1 4:41
heart rate:91 state:running today's workout:3074	Temp: 23.3°C body: 36.6°C data:2024.2.1 4:04	HUM: 36% E: 472cd data:2024.2.1 4:40
heart rate:90 state:running today's workout:2995	Temp: 23.1°C body: 36.5°C data:2024.2.1 4:03	HUM: 36% E: 463cd data:2024.2.1 4:39
heart rate:96 state:running today's workout:2918	Temp: 23.2°C body: 36.4°C data:2024.2.1 4:02	HUM: 35% E: 467cd data:2024.2.1 4:38
heart rate:89 state:running today's workout:2838	Temp: 23.3°C body: 36.4°C data:2024.2.1 4:01	HUM: 35% E: 463cd data:2024.2.1 4:37
heart rate:90 state:running today's workout:2757	Temp: 23.3°C body: 36.5°C data:2024.2.1 4:00	HUM: 34% E: 459cd data:2024.2.1 4:36
end of data		end of data

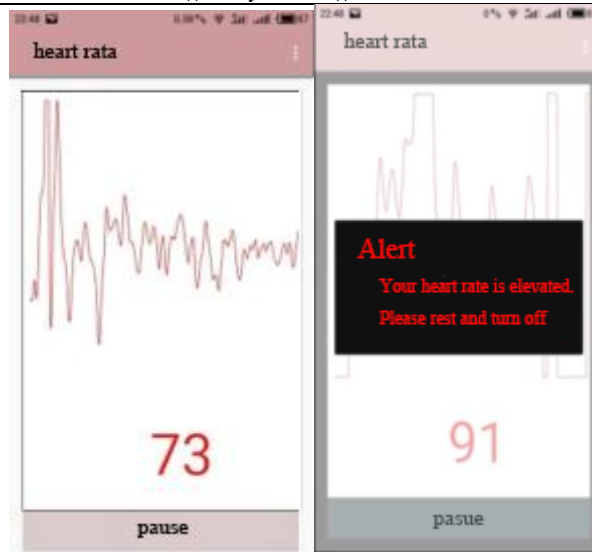
(a). HR & Exercise

(b). Temp & BT

(c). LI & Humidity

Figure 5 Initialization Page/Initialization Screen

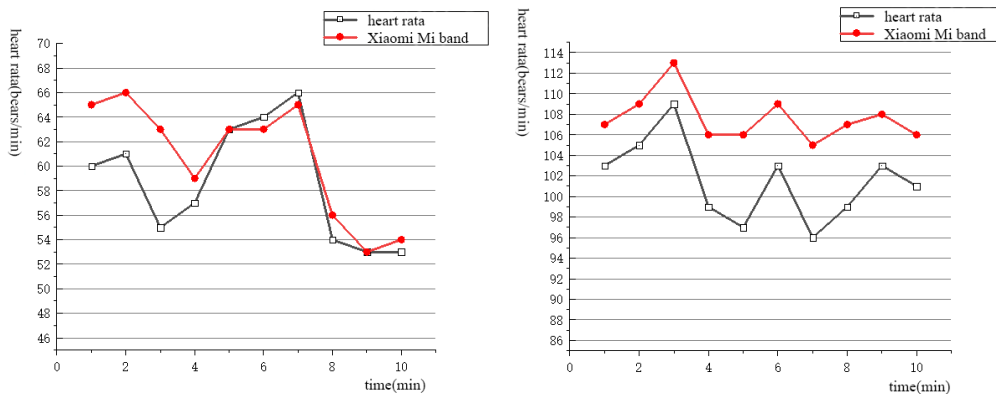
During the real-time monitoring of the system, when multiple test events were switched repeatedly, all test pages were able to navigate normally, and real-time data changes could be observed. When external conditions exceeded a certain numerical limit, a warning page popped up. By repeatedly switching between the monitoring page and the historical data display page, it was found that the data could be timely stored in the database and displayed on the page. After performing deletion operations, the data on the historical data query page could also be completely deleted, indicating that the data could be normally displayed and queried in real-time. Figure 6 illustrates the real-time refreshing of heart rate monitoring values and the popup reminder.



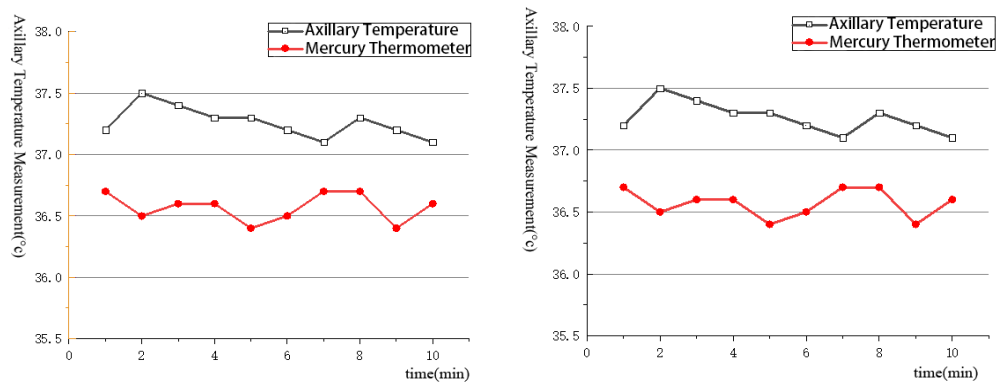
(a).Heart Rate Changes (b).Heart Rate Alert Pop-up  
 Figure 6.Heart Rate Monitoring Test

#### 4.2 Analysis of Calibration Test Results

The During the heart rate monitoring calibration test, the human body was in a resting state and a motion state, respectively. The heart rate monitoring values of the Xiaomi Mi Band 2 were used as the standard values for comparison. The numerical analysis results are presented in Figure 7. During the body temperature monitoring calibration test, the axillary and finger temperature values of the human body were monitored and compared with a medical mercury thermometer, and the results are shown in Figure 8.



(a) Resting Measurement (b) Exercise Measurement  
 Figure 7. Heart Rate Comparison Chart



(a) Axillary Temperature (b) Finger Temperature  
 Figure 8.Body Temperature Comparison Chart



As seen in Figures 6 and 7, during monitoring of the same person within the same time period, the error range of the heart rate monitoring value in the resting state compared to the Xiaomi Mi Band 2 was 1.5% to 2.4%. Under motion conditions, the fluctuation range of the monitored data was -0.8% to 3.6%. This is partly attributed to the fact that the Xiaomi Mi Band 2, being more compact, may have a different sensitivity compared to the heart rate monitoring module of our system. In the future, a more precise heart rate monitoring module can be adopted and the system's size can be reduced to achieve more accurate heart rate monitoring. In terms of body temperature monitoring, whether monitoring was done under the arm or on the finger, the values obtained were similar to those measured with a mercury thermometer. However, the time required for temperature monitoring using our physiological monitoring system is significantly faster than with a mercury thermometer, with an average test time of only 0.021s, indicating that body temperature monitoring is both accurate and quick.

## V. Conclusion

In summary, this paper combines the current research status of physiological monitoring devices both domestically and internationally to design a portable physiological monitoring system. The system utilizes the STM32F103RE as the main control chip and a variety of internal and external characteristic sensors as the data acquisition module, enabling the collection and transmission of physiological indicators and external environmental data. The software component of the physiological monitoring system features an Android-based physiological information application, which displays externally collected physiological information, such as heart rate and external light intensity, on the Android app with a popup alarm function. Comparative test results show that there is a certain error between the heart rate test and the Xiaomi Mi Band 2 test values, but it is within an acceptable range. The body temperature test is largely consistent with a medical mercury thermometer, and the test speed is faster, at only 0.021s, demonstrating real-time performance.

- (1) In data error processing, selecting gray prediction hyperparameters as the optimization target, rather than creating an objective function, involves a two-stage optimization process. The first stage involves optimizing the model, specifically the traditional mapping function. The second stage then optimizes the data itself. Compared to traditional methods of deriving various errors such as vibration errors and noise errors by creating mapping functions, the gray model does not directly yield error results. However, it is better able to demonstrate the autocorrelation and cross-correlation between data points, resulting in smoother data curves. This prepares the BP neural network for finding the parametric relationship between data and reality, while also simplifying precision control compared to directly setting the mapping function.
- (2) Compared to commonly available human characteristic monitoring bracelets on the market, the system has added the functionality of external environmental monitoring, integrating environmental and human characteristics. This allows users to more easily locate the source of abnormalities in their physiological characteristics and avoid being exposed to adverse environments for extended periods, thus minimizing the impact on their well-being.

## References

- [1]. H. Deng, C.Q. Ma. Study on the guiding significance of serum testosterone monitoring for endocrine therapy in patients with locally advanced prostate cancer[J](Journal of Clinical Urology, China 2014), 321-325.DOI:10.13201/j.issn.1001-1420.
- [2]. X.C.Li. The Current Status of Mobile Healthcare Development and Existing Issues[C](Collection of Proceedings of the Chinese Medical Association, China 2015).
- [3]. M.Li. If medication should be taken for fatty liver disease [J] (Health for Everyone, China 2014) (23):57.
- [4]. D. Dai. The Design and Implementation of Wearable ecg Monitor Device based on Bluetooth 4.0 Technology [D] (Southeast University, China 2015).
- [5]. P. Li, R. Wang and X.J.Lv: The Initial Solutions for Home-based Heal [J](China Medical Device Information, China 2011):51-53.
- [6]. H.Z. Yang, Y.X.Xu and K.Wang: Real-time Bidirectional Data Transmission Based on USB Interface [J] (Computer Engineering, China 2005), (20):223-225.
- [7]. Stefan G, Kertesz, Holt, et al. Comparing Homeless Persons' Care Experiences in Tailored Versus Nontailored Primary Care Programs[J].American Journal of Public Health, 2013, 103(2): 45-46.
- [8]. Aram S, NSumru Bayin, et al. Brain stem cells as the origin of gliomas [J].World Journal of Stem Cells, 2014,6(1):38-39.
- [9]. J.L. Bai: Design of Dynamic Electrocardiogram (ECG) Signal Analysis System [D](Central South University, China 2009).
- [10]. T.S. Ke: The Supervision of Physiological Information Based on Mobile Terminal [D] (Shandong Normal University, China 2015).